*sustainability*

MDPI

*Article*

# Exploring the Impact of Winter Storm Uri on Power Outage, Air Quality, and Water Systems in Texas, USA

**Nigus Demelash Melaku, Ali Fares * and Ripendra Awal**

Cooperative Agricultural Research Center, College of Agriculture and Human Sciences, Prairie View A&M University, Prairie View, TX 77446, USA
* Correspondence: alfares@pvamu.edu

**Abstract:** Texas was hit by a record-setting cold snap from the 14–17 February 2021 after three decades that resulted in power outages, disruption of the public water systems, and other cascading effects. This study investigates the unprecedented impact of winter storm Uri on power outages, air quality, and water systems in Texas, USA. Analysis of the Parameter Regression of Independent Slopes Model (PRISM) gridded climate data showed that the average daily freezing temperature range was 0–−19 °C on 14 February 2021, with severe levels (−17–−19 °C) occurring in the Texas High Plains. Our results showed that the extreme freezing temperature persisted from 14–17 February 2021, significantly affecting power operation and reliability, and creating power outages across Texas. Uri impacted the public water systems and air quality on time scales ranging from a few minutes to several days, resulting in 322 boiling notices. The air quality index level exceeded the standard limit by 51.7%, 61.7%, 50.8%, and 60% in Dallas–Fort Worth, Houston–Galveston, Austin, and Lubbock regions. The level of the pollutants exceeded the EPA NAAQS standard allowable limits during winter storm Uri. In general, this study gives information on the government's future preparedness, policies, communication, and response to storm impacts on vulnerable regions and communities.

**Keywords:** winter storm Uri; pollutants; cold snaps; air quality index

check for updates

**Citation:** Melaku, N.D.; Fares, A.; Awal, R. Exploring the Impact of Winter Storm Uri on Power Outage, Air Quality, and Water Systems in Texas, USA. *Sustainability* **2023**, *15*, 4173. https://doi.org/10.3390/su15054173

Academic Editors: Adam Choryński and Dariusz Graczyk

Received: 18 December 2022
Revised: 31 December 2022
Accepted: 10 January 2023
Published: 25 February 2023

**Copyright:** © 2023 by the authors. Licensee MDPI, Basel, Switzerland. This article is an open access article distributed under the terms and conditions of the Creative Commons Attribution (CC BY) license (https://creativecommons.org/licenses/by/4.0/).

## 1. Introduction

Extreme weather events are increasing in frequency and intensity globally due to climate change [1–4]. Extreme weather and climate-related heavy rainfall, floods, cyclones, extreme cold, heatwaves, and drought affect infrastructure, the economy, and the environment, leading to different results such as death, famine, displacement, and health-related issues [5].

Global warming and associated changing temperature patterns have increased mortality worldwide [6–8]. Previous cold snaps occurred in Texas in 1899, 1951, 1983, 1989, and 2011 which have affected the environment and human and ecological systems [9]. According to Doss-Gollin [9], the 1951 cold event caused a significant die-off of fish life on the shallow Gulf Coast. Uri's record-setting winter storm impacted the United States, Northern Mexico, and parts of Canada during 14–17 February 2021. This extreme weather event resulted in the deaths of 246 people and impacted more than 14.9 million people across Texas, and is considered the costliest winter storm on record with over $20 billion [10]. In 2021, the population of Texas was about 29.7 million, 89.35% of which lived in urban areas, and the rest, 10.65, lived in rural Texas [11]. The winter storm affected more than 49.5% of the state's population. The frigid temperatures disrupted clean water and energy's primary source and forced the shutdown of refineries, industries, and petrochemical facilities. The cascading failure of these interdependent systems (natural gas delivery, power plant generation, etc.) resulted in disruptions and failures in the public water system, power outages, and the release of millions of pounds of pollutants and greenhouse gases into the atmosphere [12]. Climate change exposure to extreme events associated with natural

catastrophes can affect air and water quality [13–15]. Climate change strongly affects global air quality, in which ambient air pollutants are very sensitive to extreme events [16,17]. Climate change-related air quality degradation due to pollutant emissions could significantly affect health-related issues [18].

The severe freezing temperatures forced power plants to go offline, impacting public water supply systems, home heating, businesses, and other electricity users. The winter storm Uri knocked out the fuel supply generators that use natural gas, coal, nuclear, and wind across Texas. Infrastructure systems are interconnected; thus, the failure of one system results in cascading failures of other dependent systems [5]. The power outage in Texas impacted the public water supply systems, leaving most state residents without clean water services. Factories, refineries, and industries in major cities like Dallas and Houston were forced to shut down. This unprecedented shutdown resulted in higher pollutant emissions to the atmosphere, resulting in hazardous health conditions in the impacted areas. To be prepared for the future impact of extreme events such as Uri, it is vital to assess its impact and understand its causes and effects.

Different research studies have focused on the extreme impacts of winter storm Uri on the Texas water system, health, and power infrastructures [19–22]. These studies reported that the freezing temperatures led to problems for the energy resources and water systems in Texas, including frozen water pumps at nuclear power plants, snow-covered solar panels, ice build-up on wind turbine blades, frozen coal piles, frozen cooling reservoirs for thermal power plants, and frozen natural gas gathering and distribution pipelines [20–22]. Hatchet et al. [23] investigated the health impacts of winter storm Uri that are associated with power outages. Veettil et al. [24] analyzed how Uri influenced the drought severity, soil moisture content, and vegetation cover across Texas. Kemabonta [25] explored the grid resilience analysis and planning of electric power systems. However, there is a lack of detailed spatial and temporal analysis of the interconnected impacts of the Uri on power outages, public water systems, and the associated air pollution. Hence, the objective of the study was to explore the joint and interdependent impacts of winter storm Uri on power outages, public water systems disruption, and air quality across Texas's major metropolitan areas by the time window (before, during, and after the winter storm), and to analyze the spatiotemporal distribution of the power outages, aerosol distribution and concentration, air quality indices ($PM_{2.5}$, $NO_2$, CO, and $O_3$), public water supply systems failure, and boiling water notices before, during, and after the storm.

## 2. Methodology

### *2.1. Description of the Study Area*

The study concentrated on Texas state, which was highly affected by the winter storm Uri during 14–17 February 2021. Texas has ten climate divisions with diverse geographic and climatic conditions (Table 1). The broader variation of these climate divisions results from the interaction between the geographic location and other factors such as seasonal air mass movement, tropical cyclones, and subtropical winds (Figure 1). Texas has a population of 29.7 million and comprises 254 counties, more than any other state (Figure 1).

**Table 1.** Mean Annual Precipitation, and Temperature for the ten Climate Divisions of Texas (2000–2021) (NOAA, 2021).

| Climate Divisions | Mean Precipitation (mm) | Mean Temperature (°C) | Climate Characteristics of Each Division |
|---|---|---|---|
| 1 | 460.0 | 15.5 | Continental steppe or semi-arid savanna |
| 2 | 595.8 | 17.6 | Sub-tropical steppe or semi-arid savanna |
| 3 | 897.6 | 18.6 | Sub-tropical sub-humid mixed savanna and woodlands |
| 4 | 1239.3 | 19.2 | Sub-tropical humid mixed evergreen-deciduous forestland |
| 5 | 312.2 | 18.8 | subtropical arid desert |
| 6 | 598.9 | 19.1 | Sub-tropical steppe or semi-arid brushland and savanna |
| 7 | 864.1 | 21.2 | Sub-tropical sub-humid mixed prairie, savanna, woodlands |
| 8 | 1250.7 | 21.2 | Sub-tropical humid marine prairies and marshes |
| 9 | 583.4 | 22.6 | Sub-tropical steppe or semi-arid brushland |
| 10 | 615.2 | 23.9 | Subtropical sub-humid marine |

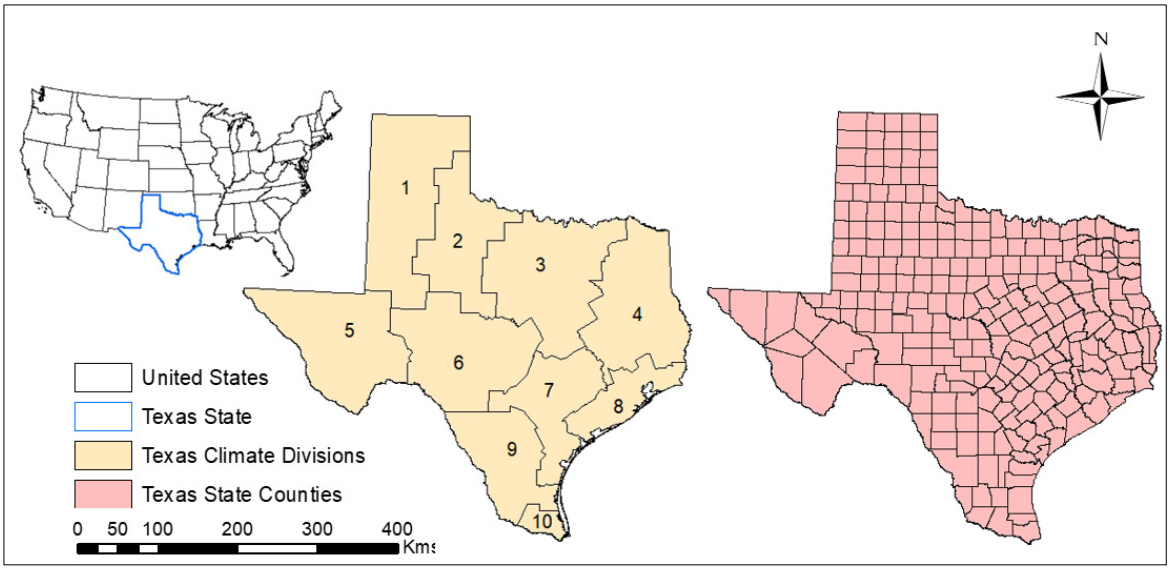



**Figure 1.** Map of the State of Texas, its ten Climate Divisions, and 254 counties that constitute the study area of this project.

### *2.2. Observation Datasets and Methods*

The daily temperature data for Texas was obtained from Parameter-Elevation Regressions on Independent Slopes Model, PRISM Climate Group, Oregon State University, http://prism.oregonstate.edu (accessed on 3 June 2021) [26]. PRISM is a climate analysis system that uses a digital elevation model (DEM), point data, and other spatial datasets to generate gridded estimates of daily, monthly, annual, and event-based climatic parameters [26]. PRISM is a knowledge-based system primarily developed to innovatively interpolate climate elements in physiographically complex landscapes. It is a unique analytical tool used extensively to map minimum temperature, maximum temperature, and precipitation over the United States. It includes vertical extrapolation of climate well beyond the highest or lowest station, reproducing gradients caused by rain shadows and coastal effects by assessing the varying impacts of terrain. The PRISM products use a weighted regression model to account for complex climate regimes associated with temperature, slope aspect, orography, rain shadows, coastal proximity, and other factors. The data sets are recognized as the highest quality spatial climate data [26]. The daily minimum temperatures during and shortly after the storm, 14–22 February 2021, were used in this analysis.

Furthermore, the hourly and daily minimum temperature data of four locations across Texas (Amarillo, Lubbock, Stephenville, and Prairie View) were obtained from the National Water and Climate Center (https://www.wcc.nrcs.usda.gov/ (accessed on 12 June 2021)) of the Natural Resources Conservation Service (NRCS) and analyzed from 14–20 February 2021. Spatiotemporal power outage data for most Texas counties during winter storm Uri were obtained from the US Power Outage website (https://poweroutage.us (accessed on 12 June 2021)), and Houston Advanced Research Center (https://harcresearch.org/ (accessed on 12 June 2021)), which monitors utility outages across the United States.

This study combined the information on the cascading impact of freezing temperatures on power outages, water treatment failures, and air pollution. Data on public water systems, boil water notices, and daily air quality and pollutant emission events during Uri resulting from the abrupt shutdowns and start-ups of industries were obtained from the Texas Commission of Environmental Quality (TCEQ; https://www.tceq.texas.gov/ (accessed on 14 June 2021)). Texas' water quality policy requires public water systems to issue boil water notices during system outages, contamination, and disinfection. This analysis used $NO_2$, CO, $O_3$, and $PM_{2.5}$ data to assess Texas' air quality indicator levels before and during Uri.

Daily spatial and temporal gridded $NO_2$ data were downloaded from NASA's Earth Data website (https://giovanni.gsfc.nasa.gov/ (accessed on 16 June 2021)). The data set contains the total column $NO_2$ for all days with less than 30 percent cloud fraction [27] based on the OMI (Ozone Monitoring Instrument) $NO_2$ algorithm version 4.0 [27,28] (Equation (1)).

$$M(z) = \frac{\int_z^\infty m(z')\alpha[T(z'), T_0]n(z^1)dz'}{\int_{z_0}^\infty n(z')dz'} \quad (1)$$

where $M$ is the air mass factor needed to compute $NO_2$ densities; $z$ is the altitude of the lower boundary of the visible part of the column; $m$ is the altitude–resolved air mass factor, $m(z')$ is the viewing geometry, which depends on the altitude $z'$ and the albedo of the lower boundary at altitude $z$, $n(z')$ is independent volume density profile for polluted air condition and $n(z')$ for unpolluted air condition; $\alpha[T(z'), T_0]$ is a factor that accounts for the temperature difference between the fitting temperature ($T_0$) and the local atmospheric temperature ($T(z')$), $dz'$ is a thin layer, and $z_0$ is the terrain height.

The carbon monoxide concentration data was also obtained from the NASA Earth Data (https://giovanni.gsfc.nasa.gov/ (accessed on 16 June 2021)). AIRS (Atmospheric Infrared Sounder) on NASA's Aqua satellite gathers daily infrared energy emitted from the Earth's surface and atmosphere globally. It provides temperature and water vapor measurements through the atmospheric column and carbon dioxide and other trace gases, including ozone, methane, and carbon monoxide. Since the AIRS main CO sensitivity is broad and centered in the mid-troposphere between approximately 300 and 600 hPa, we used the retrieved data that contains the average map of CO mole fraction at $1^\circ \times 1^\circ$ resolution with AIRS measurement of 500 hPa (500 hectopascals) [29].

The air quality index (AQI) data were obtained from the US Environmental Protection Agency (EPA). AQI is a widely used indicator that gives a timely gauge for the public on local air quality and air pollution and their impact on human health. It has a 0 to 500 scale; the higher its value, the worse the air is polluted, and consequently, the greater the health concerns are primarily for people with respiratory challenges. The air quality index scale is based on the National Ambient Quality Standards (NAAQS) [30,31] (Table 2).

**Table 2.** The U.S. National Ambient Air Quality Standards (NAAQS, https://www.epa.gov/criteria-air-pollutants (accessed on 16 June 2021)).

| AQI Level | AQI Range | $PM_{2.5}$ ($\mu g/m^3$) | $O_3$ (ppm) | $NO_2$ (ppm) | CO (ppm) | Health Recommendation |
|---|---|---|---|---|---|---|
| * Good | 0–50 * | 0–12.0 * | 0–0.054 * | 0–0.053 * | 0–4.4 * | Little or no risk |
| Moderate | 51–100 | 12.1–35.4 | 0.055–0.070 | 0.054–0.1 | 4.5–9.4 | May experience respiratory symptoms. |
| Unhealthy (sensitive) | 101–150 | 35.5–55.4 | 0.071–0.085 | 0.101–0.36 | 9.5–12.4 | Risk of experiencing irritation and respiratory problems |
| Unhealthy | 151–200 | 55.5–150.4 | 0.086–0.11 | 0.361–0.649 | 12.5–15.4 | Increased likelihood of adverse effects |
| Very unhealthy | 201–300 | 150.5–250.4 | 0.11–0.20 | 0.65–1.249 | 15.5–30.4 | Noticeably affected public (restrict outdoor activities) |
| Hazardous | 301–400 | >250.4 | >0.200 | >1.25 | >30.5 | High risk of adverse health effects |

* US Environmental Protection Agency National Ambient Quality Standards air quality limits.

The air pollutants Particulate matter ($PM_{2.5}$), nitrogen dioxide, ozone, and carbon monoxide levels are considered in the study to evaluate the air quality index. Air quality indices are calculated based on air pollutant concentration (Equation (2)). The AQI intervals are defined by breakpoints chosen to fit both the observed and health impacts.

$$AQI = \frac{I_{Hi} - I_{Lo}}{BP_{Hi} - BP_{Lo}} * (C_p - BP_{Lo}) + I_{Lo} \quad (2)$$

where $AQI$ is the air quality index for the pollutants, $C_p$ is the concentration of the pollutants; $BP_{Hi}$ is the breaking point that is greater than or equal to the concentration of the pollutants; $BP_{Lo}$ is the breaking point that is less than or equal to the concentration of the pollutants; $I_{Hi}$ is the air quality index value corresponding to $BP_{Hi}$ and $I_{Lo}$ is the air quality index value corresponding to $BP_{Lo}$.

## 3. Results

### *3.1. Daily Average Low Temperature*

The winter storm severely impacted the south-central United States, especially Texas. The severe freezing temperatures resulting from the Northern air mass blanket caused frigid temperatures in almost all counties across Texas (Figures 2 and 3). The temperature dropped by up to −18 °C in February as compared to the previous years (Figure 2) with record-setting freezing temperatures. The minimum temperature ranged from −1 to 19.5 °C in February 2018, 2019, and 2020 across Texas. The winter storm caused freezing temperatures compared to the previous years (Figure 2); these findings concur with the findings of other studies [21–25,32,33].

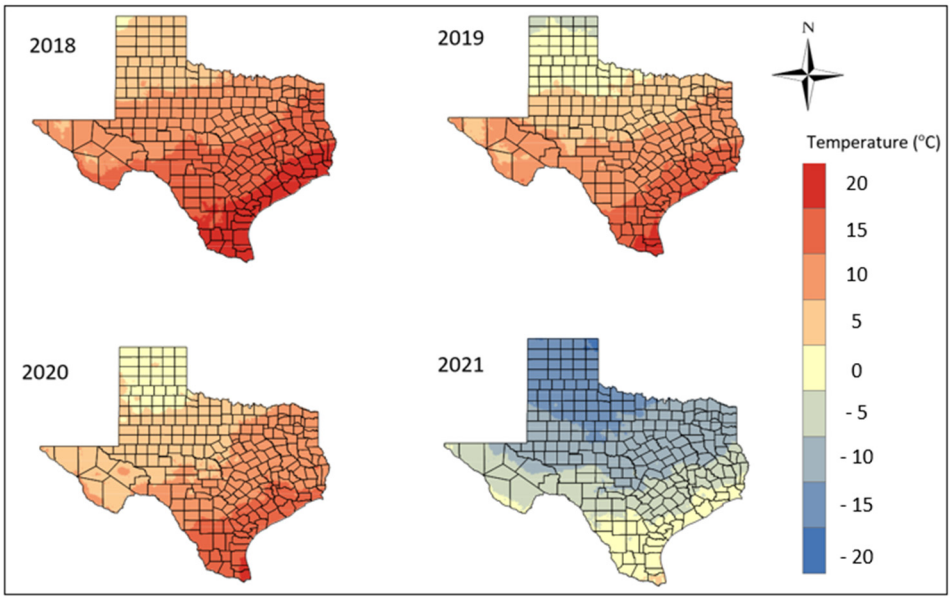



**Figure 2.** Spatio-temporal distribution of winter low-temperature records in February 2018, 2019, 2020, and 2021 in Texas.

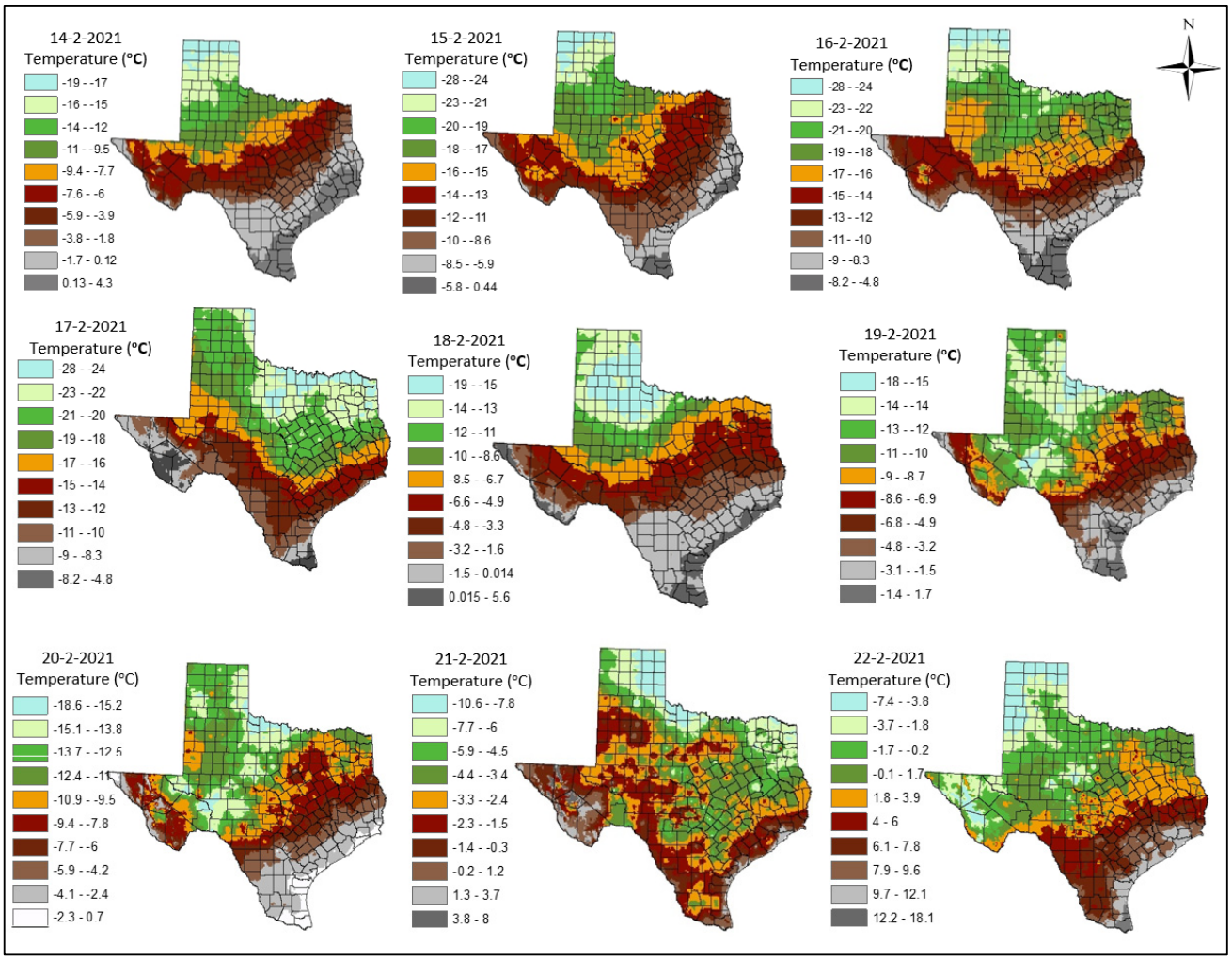



**Figure 3.** Spatio-temporal distribution of low temperatures throughout Texas during the winter Uri on 14–22 February 2021.

The PRISM spatial temperature grid showed that the average daily temperature ranged between 0 and −19 °C across Texas on 14 February 2021 (Figure 2). This extreme weather event's intensity and widespread nature had high-temperature variabilities across different parts of the state (Figure 2). The lowest temperatures were recorded in the Texas High Plains, while the relatively less severe minimum temperature was recorded in the lower valley of the state. Temperatures as low as −17–−19 °C were recorded in the Texas High Plains. The model spatial and temporal temperature grid shows a decreasing trend for the air temperature before the winter storm across Texas (Figure 3).

The widespread storm and its intensity engulfed most Texas counties to frigid temperatures for a relatively long period. Air temperatures dropped below 0 °C during 15–17 February 2021 across Texas (Figure 3). The highly severe cold temperatures occurred on 16 February 2021. The daily average low temperature increased on 21 February 2021, after the storm ended (Figure 3).

### *3.2. Cold Snap Duration*

The effects of the frigid temperatures are determined by how long those freezing temperatures persist in the area. The longer duration of the cold snap increased demands for heat and energy across the state substantially. Busby et al. [20] reported that the state of Texas was particularly hard-hit, with coincident and cascading failures of natural gas production, power generation, transportation, and water systems leaving millions of Texans without electricity, heat, and water, many for several days. The air temperatures stayed below 0 °C for five consecutive days in Amarillo, Lubbock, Stephenville, and Prairie View (Figure 4). The lowest mean hourly air temperature at Amarillo, as recorded on 15 February 2021, was −24.7 °C. The cold snaps continued for about five days, recording below 0 °C. Similarly, the lowest mean hourly air temperature reached −18.3 °C at Lubbock on 15 February 2021 for five consecutive days. The lowest mean air temperature at Stephenville and Prairie View reached −19.2 °C and −13.2 °C on 16 February 2021, respectively. The mean hourly minimum air temperature began to increase on 19 February 2021 at all four locations (Figure 4).

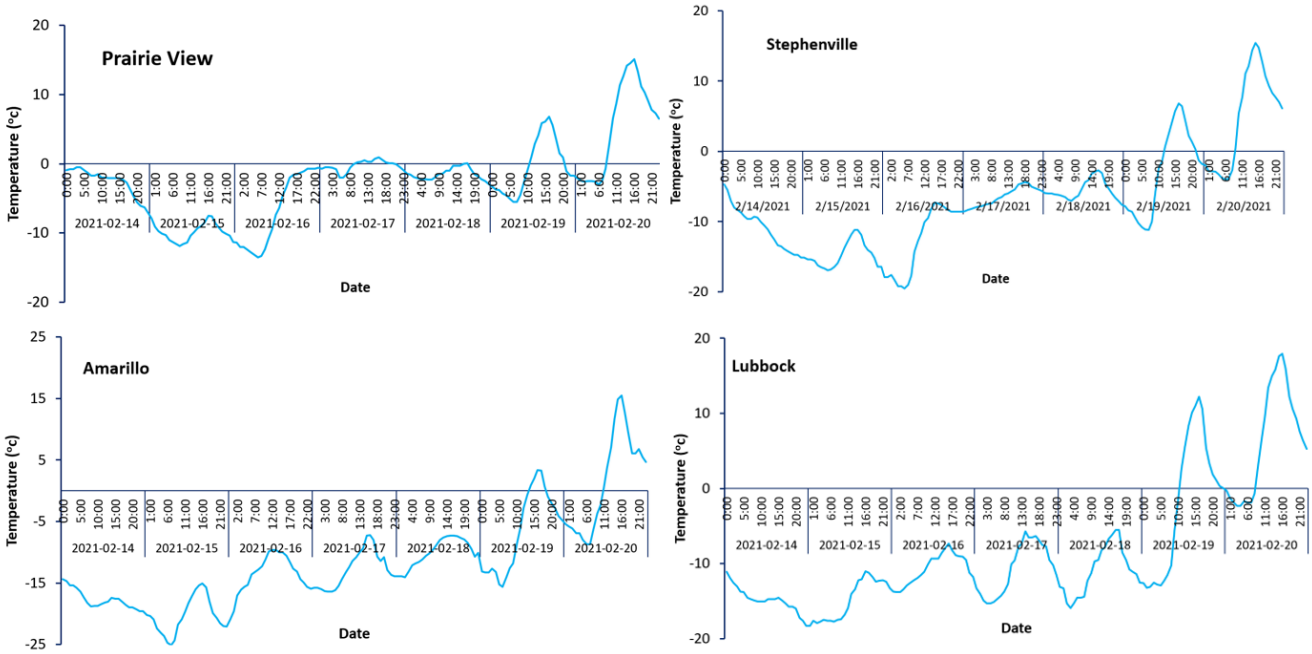



**Figure 4.** Hourly minimum temperatures over 24 h from 14–20 February 2021 at four locations in Texas.

The storm was more unusual due to the length of time temperatures remained below freezing; many stations set records with more than six consecutive days [32,34].

### *3.3. Impact of the Cold Snap Duration on Power Outages*

The power outages were unevenly spread across utilities and counties. During the onset of the winter storm on February 15, 2021, Tarrant, Dallas, and Collin counties in the Dallas-Fort Worth region experienced a total of 9,714,741 customer power outage hours, with Tarrant county accounting for 4,458,126 h, Dallas county for 3,818,191 h, and Collin county for 1,438,424 h. However, the Greater Houston–Galveston region, including Brazoria, Fort Bend, Montgomery, and Galveston counties, experienced 1,063,563 to 1,516,610 customer power outage hours.

These two major Texas metropolitan areas, Dallas–Fort Worth and Houston–Galveston regions experienced up to 7,428,422 customer power outage hours during parts of the storm duration. Cold weather affected more residents in these regions during 16–17 February 2021; they experienced the highest number of hours without power and heat across Texas. About 32 counties experienced power outages for more than 24 h per person, and eight other counties recorded outages for more than 72 h per person. The percentage of power outages per capita was longer in West Texas and the Harris County of the Greater Houston–Galveston region (Figure 5). At its peak, the winter storm Uri left millions of customers without electricity, some of whom for several days. The freeze had cascading effects on other services reliant upon electricity, e.g., drinking water treatment and medical services [12,20,21,35]. The resilience of the entire power system depends on the severity and duration of extreme weather events [3,25,36,37]. By 18 February 2021, the rate of power restoration started to increase in most affected counties. For example, the power outage rate in Harris county dropped from 7,801,887 outage hours to 1,419,054 outage hours and even less than 38,400 outage hours on 19 February 2021.

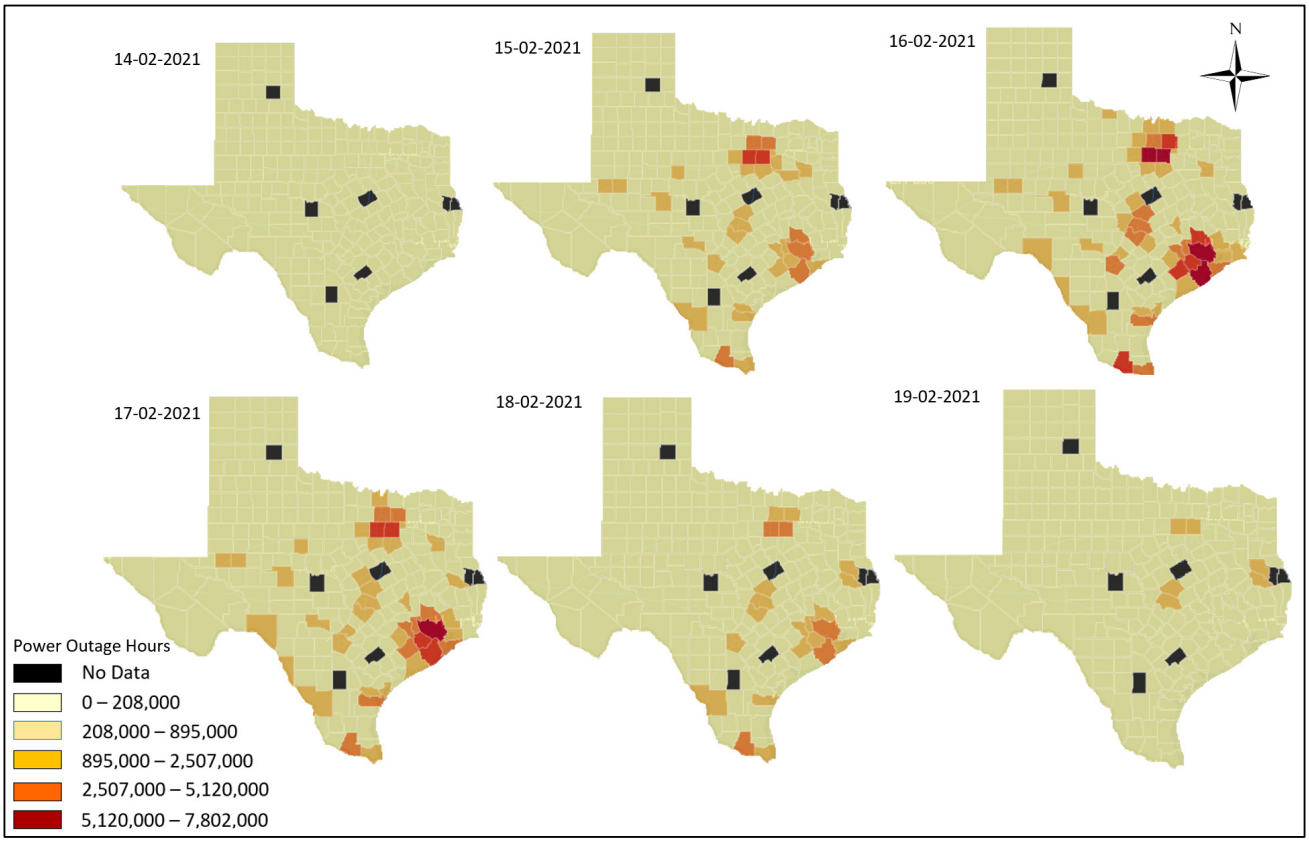



**Figure 5.** The customer power outage hours across Texas during the winter Uri, 14–19 February 2021 (Data source: PowerOutage.US).

### *3.4. Boil Water Notices*

The linkage between the interdependence of energy on one hand and water and their impact on one another was evident during the cold weather. Power sources need water in the production, extraction, cleaning, and cooling processes. In contrast, public water systems require energy to treat and distribute water. Most public water systems across Texas experience different levels of disruptions resulting in boil water notices. Many residents were advised to insulate outdoor water pipes and spigots and to drip interior faucets to prevent burst pipes in preparation for freezing temperatures. The boil water notices alert urban water consumers to boil and disinfects their drinking water due to potential health threats from contaminants, bacteria, and viruses. The Greater Houston–Galveston region has the highest boiling water notices, followed by the Dallas–Fort Worth region and other counties during extreme events (Figure 6). One survey found that 49 percent of Texans lost their running water for an average of 52 h [22]. Also, 31 percent of surveyed residents across Texas suffered water damage [22].

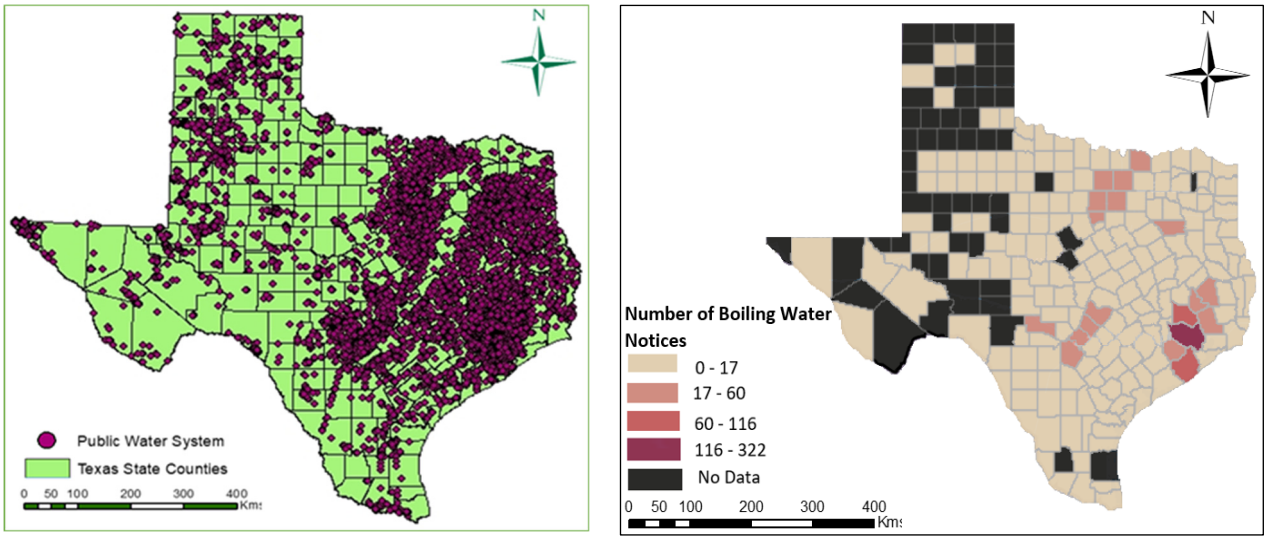



**Figure 6.** Public water systems impacted by boil water notices issued during the winter Uri (14–23 February 2021).

### *3.5. Pollutant Emission and Air Quality Impacts*

The power and energy outages due to the cold temperatures during Uri resulted in unprecedented shutdowns and start-ups in major industries, factories, and nuclear plants, causing abnormal releases of contaminants and pollutants into the environment [9]. Large amounts of pollutants were released into the atmosphere, causing a substantial increase in pollutants in the air resulting in the air quality that exceeded the standards by NAAQS across Texas during Uri. Unexpected breakdowns, maintenance, start-ups, and/or shutdown of facilities released maximum emission pollutants between the 14 and 16 February 2021 (Figure 7). The number of daily pollutant emission events increased due to Uri (Figure 7). Refineries and other petrochemical industries emitted 3.5 million pounds of excess pollution during the winter storm [35].

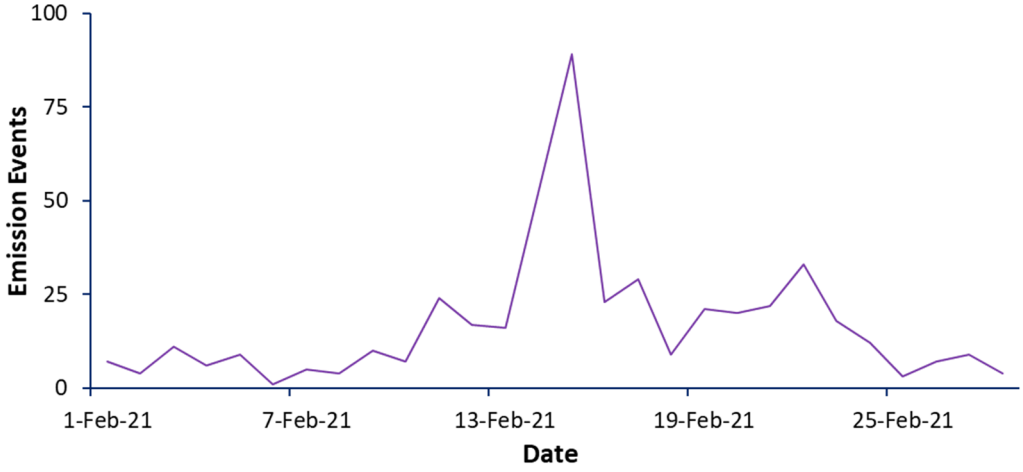



**Figure 7.** Daily pollutant emission events during February, including winter storm Uri across Texas.

During Uri, the emission events have resulted in unexpected releases of hazardous toxic chemicals and pollutants (Nitrogen dioxide, CO, and $PM_{2.5}$) emitted by factories and different industrial facilities. The spatiotemporal variation of the pollutant concentrations revealed interesting results (Figures 8 and 9).

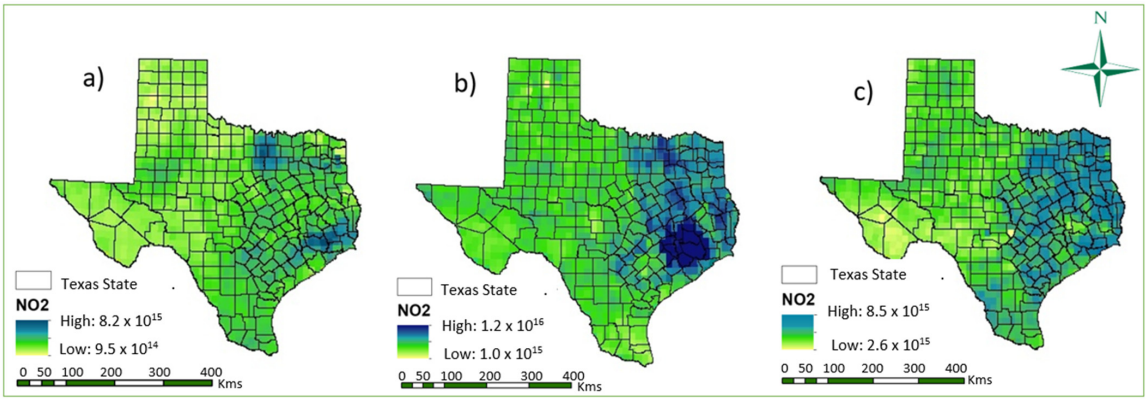



**Figure 8.** The time-averaged distribution of $NO_2$ Total Column (30% Cloud Screened) daily 0.25 deg. [OMI OMNO2d v003] $1/cm^2$. (**a**) Before winter storm Uri, (**b**) during the winter storm period, and (**c**) after the winter storm.

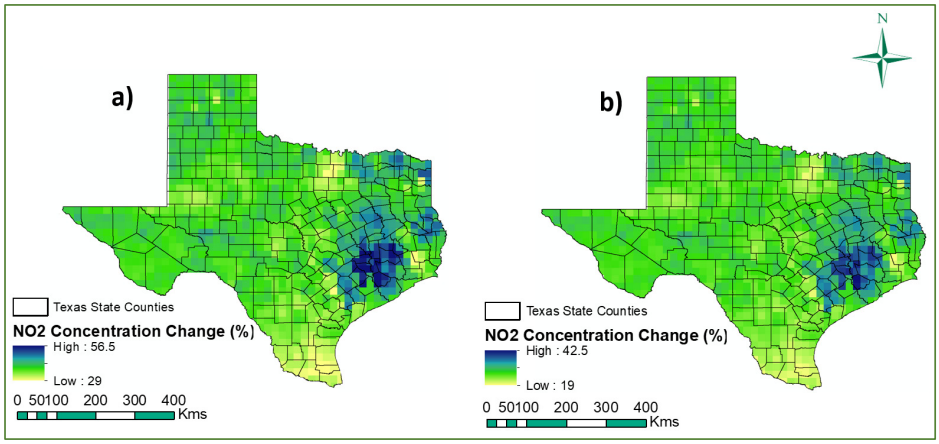



**Figure 9.** The percentage (%) change of the time-averaged distribution of $NO_2$ Total Column (30% Cloud Screened) daily 0.25 deg. [OMI OMNO2d v003] $1/cm^2$. (**a**) % change before and during winter storm Uri, (**b**) % change before and after winter storm Uri.

The data of $NO_2$ vertical columns resulting from the nitrogen oxides (NOx = $NO_2$ + NO) released before and during Uri across Texas were observed from satellite images displayed across Texas (Figure 8). The results of the spatiotemporal analysis showed that the highest observed $NO_2$ occurred during the winter storm. The air $NO_2$ concentration was higher in the Greater Houston–Galveston and Dallas–Fort Worth regions. The densities of the pollution varied across Texas. Higher pollutant emission was observed in major cities such as Dallas–Fort Worth, Greater Houston–Galveston, Austin, and Lubbock. Nearly as much air pollution was released during Hurricane Laura when facilities in the major cities of Texas reported releasing an estimated 4 million pounds of emissions [35]. At the same time, the lowest observed $NO_2$ levels occurred before Uri (Figure 8a,b). The $NO_2$ vertical columns resulted from the emissions of nitrogen oxides (NOx = NO + $NO_2$) that were formed by pollutant emissions from major industries, factories, and power plants (Figure 8). The emissions caused abnormal releases of contaminants and pollutants into the environment as they were forced to abruptly shut down their activities. $NO_2$ would be transported away from its sources, governed by the prevailing winds following its release (Figure 8c). Therefore, the $NO_2$ column amounts in the atmosphere can be highly variable and dependent on local emissions, chemistry, and transporting wind. That is the probable reason why the $NO_2$ level decreased after winter storm Uri (Figure 8c).

There were significant increases in the levels of $NO_2$ (29–56.5% as compared before Uri) during the winter storm as compared to the $NO_2$ level before Uri (Figure 9a). Similarly, the percentage change in $NO_2$ concentration was as high as 42% in major Texas metropolitan cities after the winter storm (Figure 9b). The $NO_2$ concentration remained high even after the end of Uri, with almost no significant changes, indicating that the winter storm's impact on the quality of the air persisted for a relatively long period.

The CO concentration distribution at 500 hPa (AIRSonly-AIRS AIRS3STD v006) from the time grid-average data set before, during, and after Uri 2021 is shown in Figure 10. There was an increase in the CO column concentration as shown by the AIRS (Atmospheric Infrared Sounder) observations during and after the winter storm (Figure 10b,c). During Uri, CO concentration was relatively higher in the Greater Houston–Galveston area (Figure 10b,c).

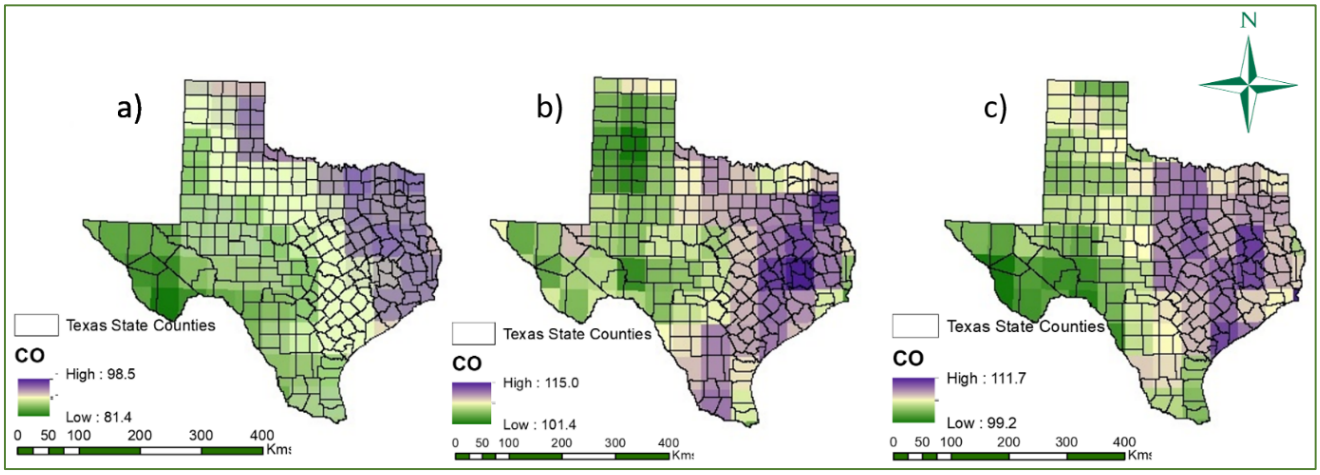



**Figure 10.** Time-averaged map of carbon monoxide, mole fraction in the air daily @500 hPa [AIRS AIRS3STD v006] ppb. (**a**) Before winter storm Uri, (**b**) during the winter storm period, and (**c**) after the winter storm.

The results of the percent (%) change (Figure 11a) show a significant increase in the levels of CO during the winter storm, as well as after the winter storm, as compared to the level before Uri. Based on the image analysis result, an increase of 7.6–24.8% was recorded during the Uri when compared with the CO concentration before Uri (Figure 11a). Similarly, the percentage change in CO concentration was as high as 20% in major metropolitan cities

after the winter storm (Figure 11b). When we compare the percent change of the CO concentration during and after Uri, the average reduction is much less, which indicates the winter storm can have longer impacts on the quality of the air.

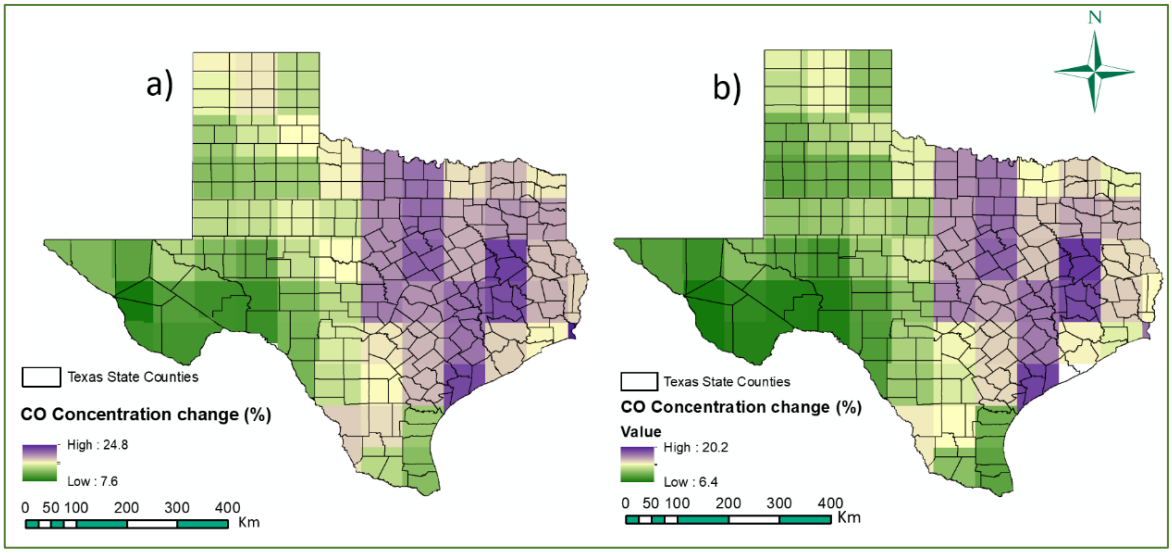



**Figure 11.** The percentage (%) change of the time-averaged map of carbon monoxide, mole fraction in air daily @500hPa [AIRS AIRS3STD v006] ppb. (**a**) % change before and during the winter storm, Uri, (**b**) % change before and after winter storm Uri.

The AQI values for the four significant locations are displayed in Figure 12. The $PM_{2.5}$ data is representative of every 24 h temporal resolution (Figure 12); however, the $O_3$, CO, and $NO_2$ data represent the average of an eight hour-period (Figures 13–15). The lower AQI values recorded before Uri started gradually increased as the storm progressed and reached its maximum level at the storm end (Figures 12–15). The higher AQI value indicates an elevated level of air pollution and more significant health risks and concerns. The lower AQI value shows a lower level of air pollution and contaminants.

Before winter storm Uri, the $PM_{2.5}$ level across the state was below the EPA primary annual standard limit (12 $\mu g/m^3$). However, the air quality degraded as the storm continued; it increased above 12 $\mu g\ m^{-3}$ and eventually exceeded the standard limit before the storm ended (Figure 12a,b). The highest $PM_{2.5}$ levels were recorded in the Dallas–Fort Worth (18.2 $\mu g/m^3$) and Greater Houston–Galveston areas (19.4 $\mu g/m^3$), Austin (18.1 $\mu g/m^3$), and Lubbock (19.2 $\mu g/m^3$). The level of $PM_{2.5}$ in these areas exceeded the EPA NAAQS air quality standard limit (Figure 12 and Table 2). The air quality index level exceeded the standard limit by 51.7%, 61.7%, 50.8%, and 60% in Dallas–Fort Worth, Houston–Galveston, Austin, and Lubbock regions. These results show that almost all of Texas had poor air quality, with levels of the major air quality pollutants exceeding the EPA NAAQS standard limits (Figure 12a,b). The air quality went from good with little or no risk (AQI level > 50) to moderate (AQI level between 50 and 100) during and following the storm as a result of the excessive releases of air pollutants during the storm.

During Uri, the mean highest $O_3$ levels were recorded in Dallas–Fort Worth, Greater Houston–Galveston, and San Antonio (Figure 13a,b). According to the results, the mean ozone level increased to 53–74% on 19 February 2021, compared to the ozone level at the beginning of the winter storm (14 February 2021) (Figure 12a,b). The mean $O_3$ levels in the Dallas–Fort Worth area were recorded at 29 ppb before the winter storm started; however, the level increased from 29 ppb to 50 ppb during the peak-storm period. Similarly, the level increased from 19 ppb to 50 ppb and 28 to 53 ppb in the Greater Houston–Galveston area and San Antonio.

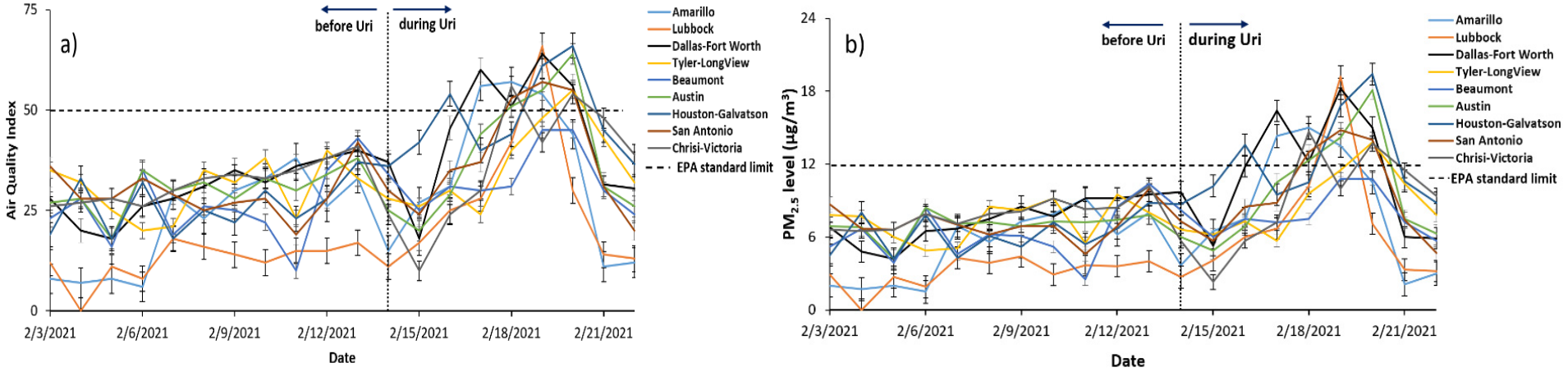



**Figure 12.** Air quality index (**a**) and particulate matter $PM_{2.5}$ level (**b**) Pre and during winter storm Uri.

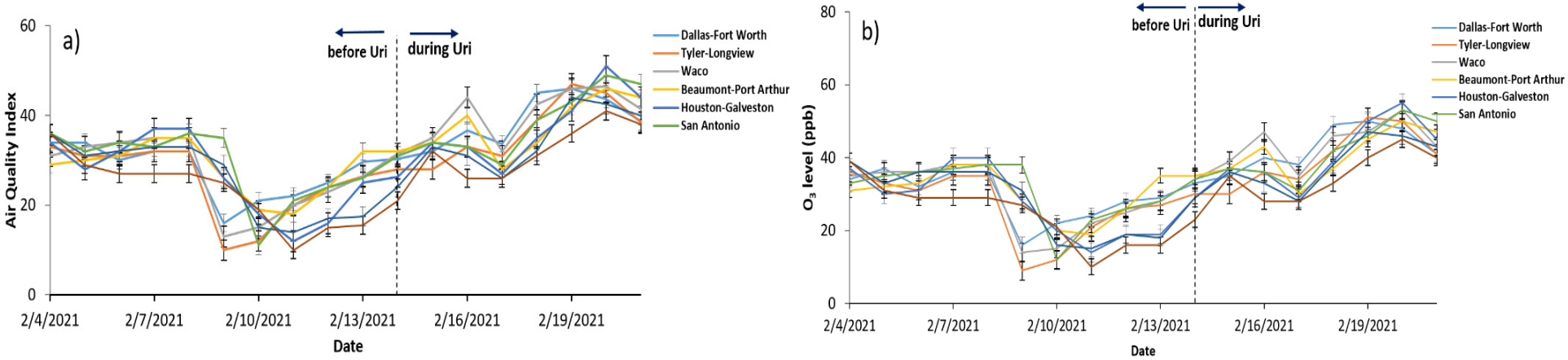



**Figure 13.** Air quality index (**a**) and ozone ($O_3$) level (**b**) pre and during winter storm Uri.

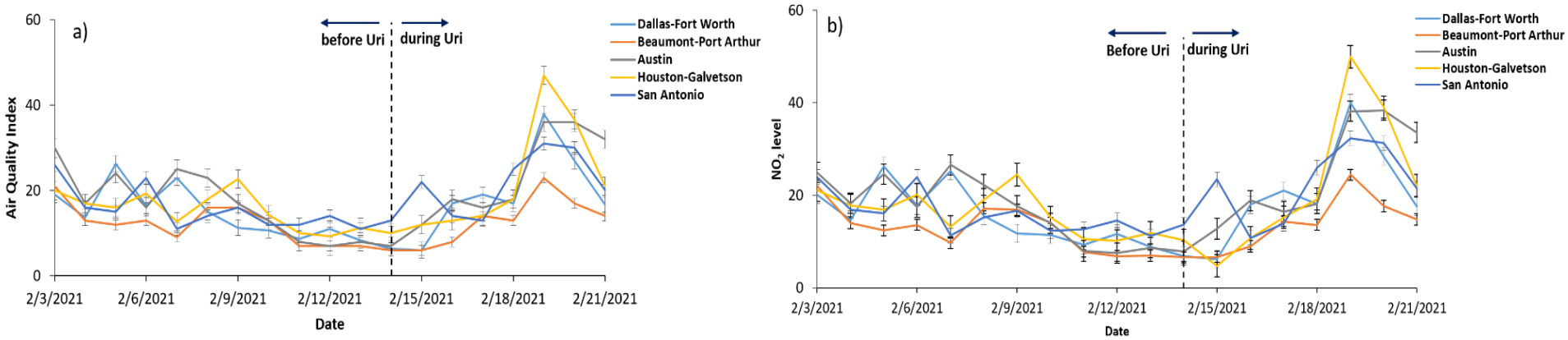



**Figure 14.** Air quality index (**a**) and nitrogen dioxide ($NO_2$) level (**b**) pre and during winter storm Uri.

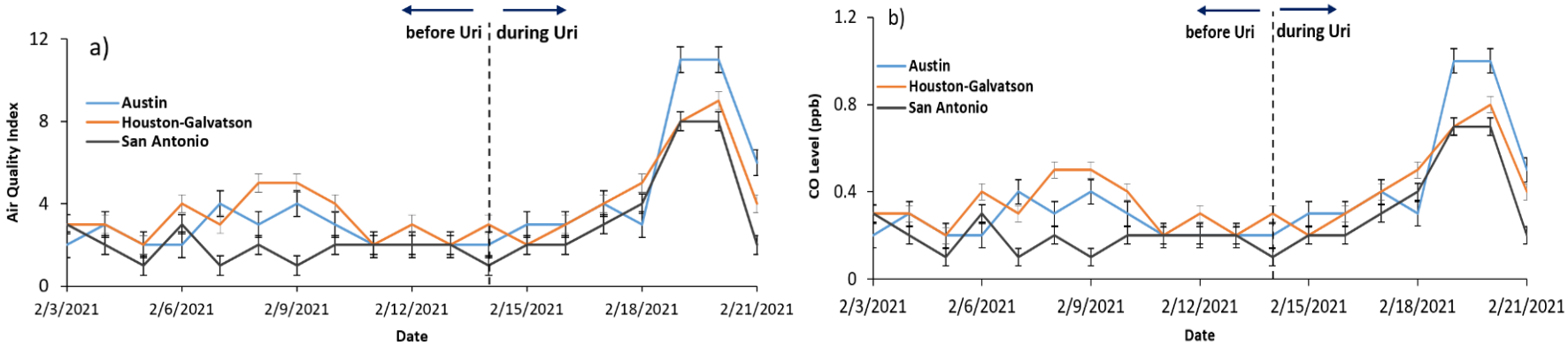



**Figure 15.** Air quality index (**a**) and carbon monoxide (CO) level (**b**) pre and during winter storm Uri.

On the other hand, the $NO_2$ levels were also higher in Dallas–Fort Worth, Greater Houston–Galveston, and San Antonio during the winter storm (Figure 12a,b). The mean $NO_2$ levels in the Dallas–Fort Worth area increased from 6.9 to 40 ppb. Similarly, in Greater Houston–Galveston and San Antonio areas, the mean $NO_2$ level increased from 10 to 50 ppb and from 13.7 to 32.4 ppb, respectively, during the winter storm.

The average highest CO levels were recorded in the Dallas–Fort Worth, Greater Houston–Galveston areas, and San Antonio during the winter storm (Figure 12a,b). The CO levels in the Dallas–Fort Worth area increased from 6.9 to 40 ppb, in the Greater Houston–Galveston area from 10 to 50 ppb, San Antonio from 13.7 to 32.4 ppb.

## 4. Discussion

The North polar vortex expanded during 2021, sending cold air southwards to the United States. Usually, this low-pressure system maintains the jet stream moving around the Earth in a circular pathway when it is healthy and strong. However, when the strong low-pressure system weakens, the jet stream does not have enough force to keep the circular travel path [38], and in 2021, it subsequently tracked the winter storm southward into the United States and became wavy and rambling [9,24]. Winter storm Uri, as a result of a polar vortex, led to below-freezing temperatures across the state of Texas. A record-setting winter storm 'Uri' draped a substantial portion of the continental U.S. from the 14–17 February [22–25,33]. The associated winter storm produced a freezing temperature from 14–17 February 2021, resulting in a cascading failure in the infrastructures that affected the Texas public and the environment [9]. Most infrastructure systems are interconnected and interlinked, resulting in a cascading failure due to power disruption during the winter storm. We found in our assessment results that the extreme freezing temperature that persists from the 14th to the 17th of February affects the operation and reliability of the power grid, creating power outages. According to Panteli and Mancarella [3], extreme weather has a significant impact on the cascading failure of infrastructures. It is considered the main cause of a wide area of energy disturbance worldwide. Extreme weather-related power interruption tends to be of high impact and sustained duration ranging from a few hours to weeks due to the severe damage inflicted on the power transmission and distribution infrastructures. Our results showed that the longer duration of the cold snap caused by the polar vortex increased demands for heat and energy across the state substantially during the winter storm. These extended freezing temperatures influenced the entire power infrastructure, resulting in extended and widespread interruption of power outages across Texas that started on 15 February 2021, 24 h after the beginning of the cold snap. This indicates that the energy system is among the critical infrastructure affected by the accumulation of ice, cold waves, and heavy snow on the overhead power lines. Under freezing conditions, ice and snow may gather on the insulators that bridge the insulators and conducting path [20].

Our result indicated that the more prolonged freezing conditions and rapid surge in energy usage caused the state's power grid began to malfunction, leading to cascading failures in the power system and widespread blackouts. The operation of energy systems such as overhead lines, generators, and transformers are governed by the permissible temperature, and thus require equipment upgrades to better withstand extreme winter temperatures. The results of this study concur with the findings of other studies that the resilience of the entire power system depends on the severity and duration of extreme weather events [3,36,37].

The winter storm also severely impacted the Texas water system. The winter causes the water to freeze and expand, leading to the destruction of the water line. Below 4 °C, the hydrogen bonds within water molecules become stronger and cause the water to expand [39]. This expansion creates very high pressure on metal and plastic water pipelines. Regardless of the strength of the container, the expanding water causes water pumps to freeze and break during extremely cold temperatures. The severe cold resulted in frozen water pumps at nuclear power plants, frozen power natural gas distribution lines, snow-

covered solar panels, ice on wind turbine blades, and frozen coal piles [20]. Hence, the interconnected failure of power and water pump disruption subsequently led to partial or complete failure of the water system in Texas. On the other hand, the water systems need power for the treatment and distribution of drinking water. It also needs the power to collect, treat, and dispose of sewage. Based on the findings, winter storm Uri significantly affected these public water supply and water treatment systems due to power outages related to freezing temperatures. Klinger et al. [40] reported that interconnected infrastructure systems have a commonly occurring cascading failure due to the loss of electricity in hospital facilities, public transportation, factories, and other facilities during extreme storms. Busby et al. [20] also reported that the freeze had cascading effects on other services reliant upon electricity, including drinking water treatment and medical services.

The winter storm Uri caused unexpected shutdowns of industries, factories, nuclear plants, and other infrastructures. The start-ups and shutdowns of these infrastructures resulted in pollutants such as $NO_2$, $CO_2$, and $PM_{2.5}$ in the air that exceeded 50–70% of the aerosol concentration of the EPA NAAQS standard limits. The rise of pollutant emissions from the biggest petrochemical complexes is the fundamental reason for the increased aerosol concentration in the atmosphere. Air pollution, characterized by the high concentration of aerosol particles [41] in an aerodynamic diameter of less than 2.5 μm ($PM_{2.5}$) concentrations, is one of the major environmental concerns during the winter storm. The dispersion of pollutants leads to increases in aerosol concentration in the lower planetary boundary layer (PBL). The PBL is inherently connected to air pollution because of the bulk of aerosols residing in the PBL and the strong interactions between aerosols and the PBL [41]. During extreme events such as winter storm Uri, the pollutant emission increases the $PM_{2.5}$ concentration, which is often associated with stable atmospheric stratification. The high concentrations of aerosols can enhance the stability of PBL and, in turn, decrease the boundary layer height (BLH) and further exacerbate air pollution. On the other hand, the decreased PBL can increase relative humidity (RH) by weakening the mixing of water vapor, facilitating the creation of aerosols that further affect the air quality. These interactions can considerably increase air pollution in Texas because Texas is the home to the largest petrochemical complexes in the United States [20]. The emission is especially strong during winter storms that result in severe pollution events where the $PM_{2.5}$ concentration in most counties in Texas was much higher than the EPA NAAQS standard limits. Winter storm Uri is one of the recent extreme events with significant emissions that caused an unprecedented release of pollutants and a high concentration of aerosols that could result in health-related issues. Other observational and modeling studies suggest that aerosol–planetary boundary layer feedback influences air quality significantly [41,42]. The high concentration of aerosols can induce a temperature inversion at the top of the PBL that is often associated with massive pollutants. A study at Galveston Bay by Du et al. [43] agrees with our findings that massive pollutants were released during storms such as Hurricane Harvey and Uri.

In general terms, our findings confirmed that the substantial releases of air pollutants during Uri resulted in substantial increases in the levels of the major air pollutants: $PM_{2.5}$, ozone, nitrogen dioxide, and carbon monoxide across Texas. These findings concur with other researchers who also reported the vital importance of understanding the cascading failures of infrastructures that extend beyond the location of extreme events to other interconnected systems of the environment [44–48].

## 5. Conclusions

This study explored the unprecedented impact of the winter storm Uri on power outages, air quality, and water systems in Texas. We investigated the cascading and interconnected failures of infrastructures and the release of pollutants during storm in Texas. The PRISM temperature data showed that the average daily temperature ranged between 0 and −19 °C across Texas on 14–17 February 2021. The analysis of the hourly temperature observations found that the February 2021 event was the record longest duration of hours

below freezing. The long extreme weather event's intensity and widespread nature had high-temperature variabilities across different parts of the state, causing a power outage, water system failures, and pollutant emissions. The level of $PM_{2.5}$ exceeded the EPA NAAQS standard limits during the winter storm. We found distinctively high pollutant emissions such as particulate matter, carbon monoxide, and nitrogen dioxide before and during the winter storm. With the increasing frequency of extreme climate change events, as projected in several recent studies, intense pollutant releases are expected to occur more frequently. We believe that this impact study results provide insights for decision-making at multiple scales to communicate and prepare ahead of extreme events to prevent cascading system failure. This study highlights the storm's impact on the most affected areas and infrastructures to increase the state's awareness of Texas's extreme weather events in the future. It will give information on infrastructure resilience, which is paramount for preventing the disruption of power systems, public water systems, and air pollution from the unprecedented impacts of winter storms. In general, this study gives information on the government's future preparedness, policies, communication, and response to storm impacts on vulnerable regions and communities.

**Author Contributions:** N.D.M.: Conceptualization, Methodology, Formal analysis, Investigation, Writing—original draft, Data curation, Visualization, Software. A.F.: Conceptualization, Writing—review and editing, Visualization, Supervision, Project administration, Funding acquisition. R.A.: Conceptualization, Data curation Writing—review and editing, Visualization, Supervision. All authors have read and agreed to the published version of the manuscript.

**Funding:** This work was supported by the Evans-Allen project (No. 1021753) from the USDA National Institute of Food and Agriculture.

**Institutional Review Board Statement:** Not applicable.

**Informed Consent Statement:** Not applicable.

**Data Availability Statement:** The data presented in this study are available on request from the corresponding author.

**Acknowledgments:** This work was supported by funding from the USDA National Institute of Food and Agriculture Evans-Allen project. We acknowledge the PRISM Climate Group, Oregon State University, Natural Resources Conservation Service (NRCS), Houston Advanced Research Center (HARC), Power outage the US, Texas Commission of Environmental Quality (TCEQ), and NASA Earth for providing the publicly available data.

**Conflicts of Interest:** The authors declare no conflict of interest.

## References

1. Stocker, T.F.; Qin, D.; Plattner, G.K.; Tignor, M.; Allen, S.K.; Boschung, J.; Nauels, A.; Xia, Y.; Bex, V.; Midgley, P.M. Climate change 2013: The physical science basis. In *Intergovernmental Panel on Climate Change, Working Group I Contribution to the IPCC Fifth Assessment Report (AR5)*; Cambridge University Press: New York, NY, USA, 2013.
2. Melillo, J.M.; Richmond, T.C.; Yohe, G.W. *Climate Change Impacts the United States. The Third National Climate Assessment*; US Global Change Research Program: Washington, DC, USA, 2014.
3. Panteli, M.; Mancarella, P. Influence of extreme weather and climate change on the resilience of power systems: Impacts and possible mitigation strategies. *Electr. Power Syst. Res.* **2015**, *127*, 259–270. [CrossRef]
4. Fares, A.; Habibi, H.; Awal, R. Extreme Events and Climate Change: A Multi-disciplinary Approach. In *Climate Change and Extreme Events*; Fares, A., Ed.; Elsevier: Amsterdam, The Netherlands, 2021; pp. 1–7. [CrossRef]
5. Bell, J.E.; Brown, C.L.; Conlon, K.; Herring, S.; Kunkel, K.E.; Lawrimore, J.; Luber, G.; Schreck, C.; Smith, A.; Christopher Uejio, C. Changes in extreme events and the potential impacts on human health. *J. Air Waste Manag. Assoc.* **2018**, *68*, 265–287. [CrossRef] [PubMed]
6. Carmona, R.; Díaz, J.; Mirón, I.; Ortiz, C.; Luna, M.; Linares, C. Mortality attributable to extreme temperatures in Spain: A comparative analysis by city. *Environ. Int.* **2016**, *91*, 22–28. [CrossRef]
7. Lee, W.; Bell, M.L.; Gasparrini, A.; Armstrong, B.G.; Sera, F.; Hwang, S.; Lavigne, E.; Zanobetti, A.; Coelho, M.D.S.Z.S.; Saldiva, P.H.N.; et al. Mortality burden of diurnal temperature range and its temporal changes: A multi-country study. *Environ. Int.* **2018**, *110*, 123–130. [CrossRef] [PubMed]

8. Borge, R.; Requia, W.J.; Yagüe, C.; Jhun, I.; Koutrakis, P. Impact of weather changes on air quality and related mortality in Spain over 25 years (1993–2017). *Environ. Int.* **2019**, *133*, 105272. [CrossRef] [PubMed]
9. Doss-Gollin, J.; Farnham, D.J.; Lall, U.; Modi, V. How unprecedented was the February 2021 Texas cold snap? *Environ. Res. Lett.* **2021**, *16*, 064056. [CrossRef]
10. Texas Department of State Health Services (DSHS, 2021). February 2021 Winter Storm-Related Deaths–Texas. Available online: https://dshs.texas.gov/updates/_MortalitySurvReport_12-30-21.pdf (accessed on 20 October 2022).
11. U.S. Census Bureau. American Community Survey 1-Year Estimates. Retrieved from Census Reporter Profile Page for Texas. 2021. Available online: https://censusreporter.org/profiles/04000US48-texas (accessed on 13 June 2021).
12. Bondank, E.N.; Chester, M.V. Infrastructure Interdependency Failures From Extreme Weather Events as a Complex Process. *Front. Water* **2020**, *2*, 21. [CrossRef]
13. IPCC. Managing the Risks of Extreme Events and Disasters to Advance Climate Change Adaptation. In *A Special Report of Working Groups I and II of the Intergovernmental Panel on Climate Change*; Field, C.B., Barros, V., Stocker, T., Qin, D., Dokken, D., Ebi, K., Mastrandrea, M., Mach, K., Plattner, G.-K., Allen, S., Eds.; Cambridge University Press: Cambridge, UK; New York, NY, USA, 2012; 582p.
14. IPCC. *Synthesis report Contribution of Working Groups I, II, and III to the Fifth Assessment Report of the Intergovernmental Panel on Climate Change Technical Report Int*; Panel on Climate Change: Geneva, Switzerland, 2014.
15. Peterson, T.C.; Karl, T.R.; Kossin, J.; Kunkel, K.; Lawrimore, J.H.; McMahon, J.R.; Vose, R.S.; Yin, X. Changes in weather and climate extremes: State of knowledge relevant to air and water quality in the United States. *J. Air Waste Manag. Assoc.* **2013**, *64*, 184–197. [CrossRef] [PubMed]
16. Westervelt, D.; Horowitz, L.; Naik, V.; Tai, A.; Fiore, A.; Mauzerall, D. Quantifying PM2.5-meteorology sensitivities in a global climate model. *Atmospheric Environ.* **2016**, *142*, 43–56. [CrossRef]
17. Chen, K.; Wolf, K.; Breitner, S.; Gasparrini, A.; Stafoggia, M.; Samoli, E.; Andersen, Z.J.; Bero-Bedada, G.; Bellander, T.; Hennig, F.; et al. Two-way effect modifications of air pollution and air temperature on total natural and cardiovascular mortality in eight European urban areas. *Environ. Int.* **2018**, *116*, 186–196. [CrossRef]
18. Stowell, J.D.; Kim, Y.-M.; Gao, Y.; Fu, J.S.; Chang, H.H.; Liu, Y. The impact of climate change and emissions control on future ozone levels: Implications for human health. *Environ. Int.* **2017**, *108*, 41–50. [CrossRef] [PubMed]
19. US Department of Energy. Extreme Cold & Winter Weather. 2021. Available online: https://www.energy.gov/sites/prod/files/2021/02/f83/TLPWHITEDOE%20Situation%20UpdateCold%20%20Winter%20Weather%236.pdf (accessed on 13 June 2021).
20. Busby, J.W.; Baker, K.; Bazilian, M.D.; Gilbert, A.Q.; Grubert, E.; Rai, V.; Rhodes, J.D.; Shidore, S.; Smith, C.A.; Webber, M.E. Cascading risks: Understanding the 2021 winter blackout in Texas. *Energy Res. Soc. Sci.* **2021**, *77*, 102106. [CrossRef]
21. O'Shea, M.; Goel, R.; Miller, R. "Breaking Down the Texas Winter Blackouts: What Went Wrong?" Wood Mackenzie. 19 March 2021. Available online: https://www.woodmac.com/news/editorial/Breaking-down-the-texas-winter-blackouts/full-report/ (accessed on 18 March 2021).
22. Glazer, Y.R.; Darrel, M.T.; Banner, J.L.; Cook, M.; Mace, R.E.; Nielsen-Gammon, J.; Grubert, E.; Kramer, K.; Stoner, M.K.; Briana, M.W.; et al. Winter Storm Uri: A Test of Texas' Water Infrastructure and Water Resource Resilience to Extreme Winter Weather Events. *J. Extrem. Events* **2021**, *8*, 2150022. [CrossRef]
23. Hatchett, B.J.; Benmarhnia, T.; Guirguis, K.; VanderMolen, K.; Gershunov, A.; Kerwin, H.; Khlystov, A.; Lambrecht, K.M.; Samburova, V. Mobility data to aid assessment of human responses to extreme environmental conditions. *Lancet Planet. Health* **2021**, *5*, e665–e667. [CrossRef]
24. Veettil, A.V.; Fares, A.; Awal, R. Winter storm Uri and temporary drought relief in the western climate divisions of Texas. *Sci. Total. Environ.* **2022**, *835*, 155336. [CrossRef]
25. Kemabonta, T. Grid Resilience analysis, and planning of electric power systems: The case of the 2021 Texas electricity crisis caused by winter storm Uri (# TexasFreeze). *Electr. J.* **2021**, *34*, 107044.
26. Daly, C.; Halbleib, M.; Smith, J.I.; Gibson, W.P.; Doggett, M.K.; Taylor, G.H.; Curtis, J.; Pasteris, P.P. Physiographically sensitive mapping of climatological temperature and precipitation across the conterminous United States. *Int. J. Clim.* **2008**, *28*, 2031–2064. [CrossRef]
27. Lamsal, L.N.; Nickolay, A.K.; Marchenko, S.V.; Celarier, E.A.; Bucsela, E.J.; Swartz, W.H. OMI/Aura NO2 Cloud-Screened Total and Tropospheric Column L3 Global Gridded 0.25-degree × 0.25-degree V3, NASA Goddard Space Flight Center, Goddard Earth Sciences Data and Information Services Center (GES DISC). 2019. Available online: https://disc.gsfc.nasa.gov/datasets/OMNO2d_003/summary (accessed on 19 June 2021).
28. Palmer, P.I.; Jacob, D.J.; Fiore, A.M.; Martin, R.V. Air mass factor formulation for spectroscopic measurements from satellites: Application to formaldehyde retrievals from the Global Ozone Monitoring Experiment. *J. Geophys. Res.* **2001**, *106*, 14539–14550. [CrossRef]
29. Kahn, B.H.; Irion, F.W.; Dang, V.T.; Manning, E.M.; Nasiri, S.L.; Naud, C.M.; Blaisdell, J.M.; Schreier, M.M.; Yue, Q.; Bowman, K.W.; et al. The Atmospheric Infrared Sounder version 6 cloud products. *Atmos. Meas. Technol.* **2014**, *14*, 399–426. [CrossRef]
30. US EPA. National Ambient Air Quality Standards. Available online: https://www.epa.gov/criteria-airpollutants/naaqs-table (accessed on 7 July 2021).
31. Habibi, H.; Awal, R.; Fares, A.; Ghahremannejad, M. COVID-19 and the Improvement of the Global Air Quality: The Bright Side of a Pandemic. *Atmosphere* **2020**, *11*, 1279. [CrossRef]

32. Bolinger, R.A.; Brown, V.M.; Fuhrmann, C.M.; Gleason, K.L.; Joyner, T.A.; Keim, B.D.; Lewis, A.; Nielsen-Gammon, J.W.; Stiles, C.J.; Tollefson, W.; et al. An assessment of the extremes and impacts of the February 2021 South-Central U.S. Arctic outbreak, and how climate services can help. *Weather. Clim. Extrem.* **2022**, *36*, 100461. [CrossRef]
33. Homayoun, T.; Trackers, T.T.N.; Fuller, N.; Hensley, C. Impacts of Winter Storm Uri on Texas Fish and Wildlife. 2021. Available online: https://nri.tamu.edu/media/3131/tmn-tuesdays-newsletter-1.pdf (accessed on 7 July 2021).
34. Bertrand, D.; Speizer, S. February 2021: Extreme Cold, Snow, and Ice in the South-Central U.S. Southern Climate Impacts Planning Program. *Tech. Rep.* 2021. Available online: http://www.southernclimate.org/documents/Feb2021ExtremeCold.pdf (accessed on 7 July 2021).
35. Douglas, E. Power Companies Required to Better Prepare Plants for Winter in First Phase of Rule Approved by Texas Regulators. 2021. Available online: https://www.texastribune.org/2021/10/21/texas-power-companies-winter-weather-rule/ (accessed on 9 July 2021).
36. Ward, D.M. The effect of weather on grid systems and the reliability of electricity supply. *Clim. Chang.* **2013**, *121*, 103–113. [CrossRef]
37. Bell, J.E.; Herring, S.C.; Jantarasami, L.; Adrianopoli, C.; Benedict, K.; Conlon, K.; Escobar, V.; Hess, J.; Luvall, J.; Garcia-Pando, C.P.; et al. *Impacts of Extreme Events on Human Health in the Impacts of Climate Change on Human Health in the United States: A Scientific Assessment*; U. S. Global Change Research Program: Washington, DC, USA, 2016. [CrossRef]
38. Lillo1, S.P.; Cavallo, S.M.; David BParsons, D.B.; Christopher Riedel, C. The Role of a Tropopause Polar Vortex in the Generation of the January 2019 Extreme Arctic Outbreak. *J. Atmos. Sci.* **2019**, *78*, 2801–2821. [CrossRef]
39. Powell-Palm, M.J.; Rubinsky, B.; Sun, W. Freezing water at constant volume and under confinement. *Commun. Phys.* **2020**, *3*, 1–8. [CrossRef]
40. Klinger, C.; Landeg, O.; Murray, V. Power Outages, Extreme Events, and Health: A Systematic Review of the Literature from 2011–2012. *PLoS Curr.* **2014**, *6*. [CrossRef]
41. Li, Z.; Guo, J.; Ding, A.; Liao, H.; Liu, J.; Sun, Y.; Wang, T.; Xue, H.; Zhang, H.; Zhu, B. Aerosol and boundary-layer interactions and impact on air quality. *Natl. Sci. Rev.* **2017**, *4*, 810–833. [CrossRef]
42. Yu, H.; Liu, S.C.; Dickinson, R.E. Radiative effects of aerosols on the evolution of the atmospheric boundary layer. *J. Geophys. Res. Atmos.* **2002**, *107*, AAC-3. [CrossRef]
43. Du, J.; Park, K.; Yu, X.; Zhang, Y.J.; Ye, F. Massive pollutants released to Galveston Bay during Hurricane Harvey: Understanding their retention and pathway using Lagrangian numerical simulations. *Sci. Total. Environ.* **2020**, *704*, 135364. [CrossRef]
44. Beatty, M.E.; Phelps, S.; Rohner, C.; Weisfuse, I. Blackout of 2003: Public health effects and emergency response. *Public Health Rep.* **2006**, *121*, 36–44. [CrossRef] [PubMed]
45. Freese, J.; Richmand, N.J.; Silverman, R.A.; Braun, J.; Kaufman, B.J.; Clair, J. Impact of Citywide Blackout on an Urban Emergency Medical Services System. *Prehospital Disaster Med.* **2006**, *21*, 372–378. [CrossRef]
46. Klein, K.R.; Herzog, P.; Smolinske, S.; White, S.R. Demand for poison control center services "surged" during the 2003 blackout. *Clin. Toxicol.* **2007**, *45*, 248–254. [CrossRef] [PubMed]
47. Lin, S.; Fletcher, B.A.; Luo, M.; Chinery, R.; Hwang, S.-A. Health Impact in New York City during the Northeastern Blackout of 2003. *Public Health Rep.* **2011**, *126*, 384–393. [CrossRef] [PubMed]
48. Anderson, G.B.; Bell, M.L. Lights out: Impact of the August 2003 power outage on mortality in New York, NY. *Epidemiol. Camb. Mass* **2012**, *23*, 189–193. [CrossRef] [PubMed]


**Disclaimer/Publisher's Note:** The statements, opinions and data contained in all publications are solely those of the individual author(s) and contributor(s) and not of MDPI and/or the editor(s). MDPI and/or the editor(s) disclaim responsibility for any injury to people or property resulting from any ideas, methods, instructions or products referred to in the content.